Computer Physics Communications 121–122 (1999) 376–381

Computer Physics Communications

www.elsevier.nl/locate/cpc

Microscopic models of traveling wave equations

Eric Brunet [1], Bernard Derrida [2]

Laboratoire de Physique Statistique, ENS, 24 rue Lhomond, 75005 Paris, France [3]

Abstract

Reaction-diffusion problems are often described at a macroscopic scale by partial derivative equations of the type of the Fisher or Kolmogorov–Petrovsky–Piscounov equation. These equations have a continuous family of front solutions, each of them corresponding to a different velocity of the front. By simulating systems of size up to $N = 10^{16}$ particles at the microscopic scale, where particles react and diffuse according to some stochastic rules, we show that a single velocity is selected for the front. This velocity converges logarithmically to the solution of the F-KPP equation with minimal velocity when the number N of particles increases. A simple calculation of the effect introduced by the cutoff due to the microscopic scale allows one to understand the origin of the logarithmic correction.

1. The Fisher equation

The Fisher equation [1], also called KPP equation (for Kolmogorov–Petrovsky–Piscounov [2]) is widely used to describe front propagation in many problems of physics, chemistry and biology:

$$\frac{\partial c}{\partial t} = \frac{\partial^2 c}{\partial x^2} + c - c^2. \tag{1}$$

Fisher first introduced this equation to represent "The Wave of Advance of Advantageous Genes" [1] in a population. The concentration $c(x,t)$ was the fraction of individuals in a population at position x and time t that exhibit some benefit genes, and (1) was used to describe how this favorable gene would spread in the population. Eq. (1) can also model the dynamics of sick individuals in a population during a viral contagious infection, the proportion of burnt-out gases in a combustion [3], the concentration of some species produced in a chemical reaction, etc. It also appears in the mean field theory of directed polymers in a random medium [4] and in the calculation of Lyapunov exponents of large sparse random matrices [5,6].

In (1), $c(x,t)$ represents a concentration, implying that, for all x and t:

$$0 \leqslant c(x,t) \leqslant 1. \tag{2}$$

If we look at solutions constant in space ($\partial c/\partial x = 0$), Eq. (1) becomes simply:

$$\frac{\partial c}{\partial t} = c - c^2. \tag{3}$$

There are two stationary solutions: $c = 0$ (unstable fixed point) and $c = 1$ (stable fixed point).

The role of the diffusion term $\partial^2 c/\partial x^2$ in (1) is to spread any positive perturbation. Therefore, if initially $c(x,0) > 0$ in some region of space and $c(x,0) = 0$ elsewhere, the perturbation will grow, reach asymptotically the stable fixed point $c = 1$ and spread throughout the whole space. Ultimately, the stable value $c = 1$ will be reached everywhere.

[1] E-mail: eric.brunet@ens.fr.

[2] E-mail: bernard.derrida@ens.fr.

[3] Laboratoire associé au CNRS et aux Universités Paris VI et Paris VII.

0010-4655/99/$ – see front matter
PII: S0010-4655(99)00358-6

To study how the stable region (where $c = 1$) invades the unstable one (where $c = 0$), one can consider an initial condition where $c(x, 0)$ decreases monotonically from $c(-\infty, 0) = 1$ to $c(+\infty, 0) = 0$. If at time $t = 0$ the initial condition $c(x, 0)$ decreases fast enough as $x \to \infty$ (in particular if $c(x, 0)$ is a step function), the front moves in the long time limit with a well defined speed $v_{\min}$ [7]:

$$v_{\min} = 2. \tag{4}$$

To understand from (1) why the velocity $v_{\min} = 2$ is selected looks a priori a very hard task. Eq. (1) is a non-linear partial derivative equation and there is no way of writing the full expression of $c(x, t)$ for an arbitrary initial condition. However, the velocity $v_{\min} = 2$ can be understood easily without solving the full non-linear problem: let us assume that the front moves at some constant speed v. The concentration profile $c(x, t)$ takes then the form:

$$c(x, t) = F_v(x - vt), \tag{5}$$

where $F_v(z)$ is the solution of:

$$F_v'' + vF_v' + F_v - F_v^2 = 0 \tag{6}$$

with $F_v(-\infty) = 1$ and $F_v(+\infty) = 0$. In the region where $F_v(z) \ll 1$, i.e. far ahead of the front, one can neglect in (6) the non-linear term. The general solution of the linearized equation is a sum of two exponentials so that for $z \to +\infty$ one of these two exponentials dominates:

$$F_v(z) \simeq Ae^{-\gamma z}, \tag{7}$$

and, from the linearized version of (6), one finds that v and γ are related by:

$$v(\gamma) = \gamma + \frac{1}{\gamma}. \tag{8}$$

We see that the asymptotic decay γ in (7) determines completely the velocity $v(\gamma)$ of the front.

What (8) tells us is that any velocity $v \geqslant v_{\min}$ ($v_{\min} = 2$) is possible for the front. (It should be noted that $v < v_{\min}$ would also be possible by allowing γ to be complex. However, a front moving at such a speed would take negative values in the tail, and this would violate condition (2).)

The minimal speed $v_{\min} = 2$ reached for $\gamma_{\min} = 1$ has a special status: it has been shown [8–12] that if in its initial condition the front decays faster than $e^{-\gamma_{\min} x}$ (in particular, if $c(x, 0)$ is a step function), then the front moves asymptotically with this minimal speed $v_{\min}$. Moreover, in the long time limit, the position $X(t)$ of the front is given by

$$X(t) = 2t - \frac{3}{2}\ln t + O(1). \tag{9}$$

(In other words, the velocity of the front converges to $v_{\min} = 2$ with a leading correction [12] given by $-3/(2t)$. The presence of a logarithmic correction in (9) makes often a precise determination of the asymptotic velocity difficult.)

Most properties of (1) (selection of the minimal velocity for steep enough initial conditions, logarithmic corrections to the position as in (9)) can also be recovered in a whole class [10] of front equations where a stable region invades an unstable one. An example very different from (1) that we will consider below is:

$$c(x, t+1) = 1 - \left[1 - \int d\alpha\, \rho(\alpha) c(x - \alpha, t)\right]^2, \tag{10}$$

where $\rho(\alpha)$ can be any density function ($\rho(\alpha) \geqslant 0$ and $\int d\alpha\, \rho(\alpha) = 1$). As for (1), the uniform solutions $c = 0$ and $c = 1$ are respectively unstable and stable and the integral over α spreads any positive perturbation as does the diffusion term in (1).

As for (1), the linearized version of (10) where terms quadratic in c are neglected determines the velocity. For an exponential decay (7) of the front, one finds a dispersion relation $v(\gamma)$ generalizing (8):

$$v(\gamma) = \frac{1}{\gamma}\ln\left[2\int d\alpha\, \rho(\alpha) e^{\gamma\alpha}\right], \tag{11}$$

and for a steep enough initial condition the minimum velocity

$$v_{\min} = \min_{\gamma} v(\gamma) = v(\gamma_{\min}) \tag{12}$$

is reached in the long time limit. The position $X(t)$ is then given [11] for large t by:

$$X(t) = v_{\min} t - \frac{3}{2\gamma_{\min}}\ln t + O(1). \tag{13}$$

(Note that in general $\gamma_{\min}$ in (12) is finite except for very particular choices of $\rho(\alpha)$.)

2. The microscopic stochastic model

Front equations of type (1) or (10) originate often as the large-scale limit of microscopic stochastic mod-

els [3,5,6,13–15]. Here we study a particular microscopic model which, as we will see, is described in the large scale limit by the front Eq. (10). We will compare the velocity measured for this microscopic stochastic problem with the velocity (11), (12) expected for the traveling wave Eq. (10).

Our microscopic model [11] is defined as follows: Imagine a population where each generation has exactly N individuals. Each individual i ($1 \leqslant i \leqslant N$) at generation t (t is an integer) is characterized by its fitness $x_i(t)$, a real number representing its adaptation to the environment. The state of the system at any time t is completely determined by the N numbers $x_i(t)$.

At time $t = 0$, we set $x_i(0) = 0$ for all i (but this choice of initial condition is actually unimportant in the long-time limit). By definition of the model, the $x_i(t)$ evolve from generation t to generation $t+1$ with the following rule:

$$x_i(t+1) = \max\bigl[x_{m_i}(t) + \alpha_i,\, x_{f_i}(t) + \alpha_i'\bigr], \tag{14}$$

where m_i and f_i are the two parents of the new individual i, chosen at random in the previous generation t (in other words, m_i and f_i are random integers uniformly distributed between 1 and N), and where α_i and α_i' are random numbers independently chosen according to some probability distribution $\rho(\alpha)$ representing random mutations. So at each generation, the m_i, f_i, α_i and α_i' are independent and new values are chosen at every time step.

Under the dynamics (14), the cloud of N points $x_i(t)$ moves along the line and we want to determine its asymptotic velocity v_N, that is:

$$v_N = \lim_{t\to+\infty} \frac{X(t)}{t}, \tag{15}$$

where

$$X(t) = \frac{1}{N}\sum_{i=1}^{N} x_i(t). \tag{16}$$

Let us now see how one can relate this microscopic model to the traveling wave equation (10). We define $c(x,t)$ as the fraction of population which has a fitness larger than x:

$$c(x,t) = \frac{1}{N}\sum_{i=1}^{N} \Theta\bigl(x_i(t) - x\bigr). \tag{17}$$

(By convention, we choose here $\Theta(x) = 1$ if $x > 0$ and $\Theta(x) = 0$ if $x \leqslant 0$.) Obviously, $c(x,t)$ is a monotonic decreasing function of x going from $c(-\infty,t) = 1$ to $c(+\infty,t) = 0$. At time $t = 0$, we have $c(x,0) = 1$ for $x < 0$ and $c(x,0) = 0$ for $x \geqslant 0$, so the initial condition is a step function. It should be noted that $c(x,t)$ can only take values which are integral multiples of $1/N$.

Clearly from (17), the position $X(t)$ of the cloud of points can be rewritten with the function $c(x,t)$ as:

$$X(t) = X(0) + \int_{-\infty}^{+\infty} dx\,\bigl[c(x,t) - c(x,0)\bigr]. \tag{18}$$

Given the positions $x_i(t)$ of all the particles (or, equivalently given the function $c(x,t)$), the $x_i(t+1)$ obtained from (14) are independent random variables. Therefore, if we fix $c(x,t)$, the average $\langle c(x,t+1)\rangle$ over the dynamics between time t and $t+1$ gives:

$$\bigl\langle c(x,t+1)\bigr\rangle = 1 - \Bigl[1 - \int d\alpha\,\rho(\alpha) c(x-\alpha,t)\Bigr]^2, \tag{19}$$

which, except for the $\langle\ \rangle$, is exactly (10). However, if we try to average over the whole history (i.e. over all the timesteps), we need to average terms quadratic in c on the right hand side of (19). This means $\langle c(x,t+1)\rangle$ is not only related to $\langle c(x,t)\rangle$, but also to correlations like $\langle c(x,t)c(x',t)\rangle$, and this makes the problem very difficult for finite N. On the other hand, if we neglect these correlations (and one can argue that these correlations are small for large enough N) and replace $\langle c(x,t)c(x',t)\rangle$ with $\langle c(x,t)\rangle\langle c(x',t)\rangle$, then (19) reduces exactly to (10). So (10) can be thought as the mean-field (or large N) version of the microscopic model (14).

As the initial condition $c(x,0)$ given by (17) is a step function, the mean field equation predicts a front moving at the minimum velocity $v_{\min}$ given by (11), (12).

3. Direct simulations

We have simulated the microscopic model (14) for several choices of the distribution $\rho(\alpha)$: the uniform distribution in the range $0 \leqslant \alpha \leqslant 1$

$$\rho_{\text{uni}}(\alpha) = \Theta(\alpha)\Theta(1-\alpha), \tag{20}$$

Table 1
Values of $\gamma_{\min}$ and $v_{\min}$ for different models

Model	$\rho = \rho_{\text{uni}}$	$\rho = \rho_{\text{exp}}$	$\rho = \rho_{\text{disc}}$	Martian model
$\gamma_{\min}$	5.262 076...	0.626 635...	2.553 245...	8.133 004...
$v_{\min}$	0.815 172...	2.678 347...	0.810 710...	0.877 338...

the exponential distribution

$$\rho_{\text{exp}}(\alpha) = \Theta(\alpha) e^{-\alpha}, \tag{21}$$

and a discrete distribution

$$\rho_{\text{disc}}(\alpha) = 0.25\,\delta(1-\alpha) + 0.75\,\delta(\alpha). \tag{22}$$

We have also simulated a generalization of the problem (Martian genetics) where each new individual at time $t+1$ has *three* parents, so that (14) is replaced by the max over three terms, with the effect of mutations distributed according to (20).

The minimal value of the speed $v_{\min}$ and the corresponding decay rate $\gamma_{\min}$ of the deterministic front equations (10)–(12) for these four cases are given in Table 1.

For these four models, we have simulated (14) for $T = 10^7$ timesteps after a transient time of $T' = 10^6$ timesteps to eliminate the effect of initial conditions. For several choices of N, we have measured the speed as:

$$v_N = \frac{X(T+T') - X(T')}{T}. \tag{23}$$

Fig. 1 represents the difference between the mean-field speed $v_{\min}$ (given in Table 1) and the speed v_N measured in the simulation for several choices of N (16, 32, 64, 128, 256, 512, 1024, 2048 and 4096).

We see in Fig. 1 that a single speed v_N is selected in the microscopic model. This speed is always lower than the speed $v_{\min}$ of the deterministic front equation, and the difference $v_{\min} - v_N$ seems to decay like $N^{-1/3}$ for all the variants of the model. The effective power law exponent seems however to decrease slowly as N increases.

In order to confirm the $N^{-1/3}$ decay of Fig. 1, we tried to increase N, but as in the direct simulation computer time scales like $N \times T$, it is very hard to make N much larger than 10^4 or 10^5 for a number $T = 10^7$ of timesteps.

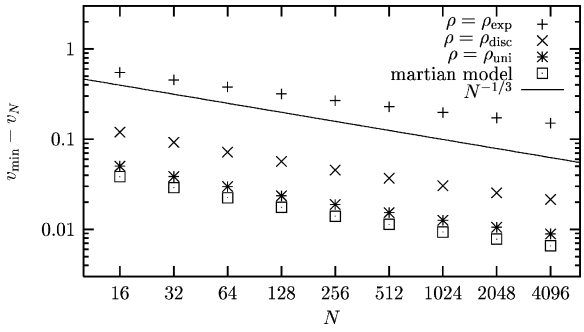

Fig. 1. Log–log plot of the difference between the speed $v_{\min}$ given by the mean-field theory and the speed v_N measured in Monte Carlo simulations for the four models as a function of the number N of particles. The straight line represents $N^{-1/3}$.

4. Highly parallel simulations

We are now going to describe a computational trick which we developed [11] for some particular distributions $\rho(\alpha)$ such as

$$\rho(\alpha) = p\delta(\alpha - 1) + (1-p)\delta(\alpha), \tag{24}$$

allowing to simulate the microscopic model for a huge number of points (N up to 10^{16}). We restrict p to the range $0 < p < 0.5$ (to avoid one of the rare cases where (11) has no minimum for a finite $\gamma_{\min}$).

For the distribution (24), the $x_i(t)$ are always integers if they are so at $t = 0$ and the concentration $c(x,t)$ as defined by (17) is constant between any pair of consecutive integers. We call respectively $x_{\min}$ and $x_{\max}$ the positions of the leftmost and rightmost particles at time t and $w = x_{\max} - x_{\min} + 1$ the width of the front. We observed in our simulations that w is typically of order $\ln N$, so that even for N as huge as 10^{16}, the number of possible values of the $x_i(t)$ at a given time is very limited, and the whole information in $c(x,t)$ is carried by the number of particles at each integer x between $x_{\min}$ and $x_{\max}$.

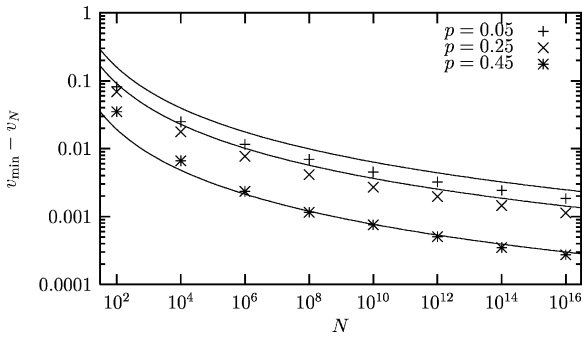

Fig. 2. Differences between the speed obtained by the mean-field theory and the speed measured in highly parallel simulations for different values of p as a function of the number N of particles. The lines represent for each value of p the prediction (27).

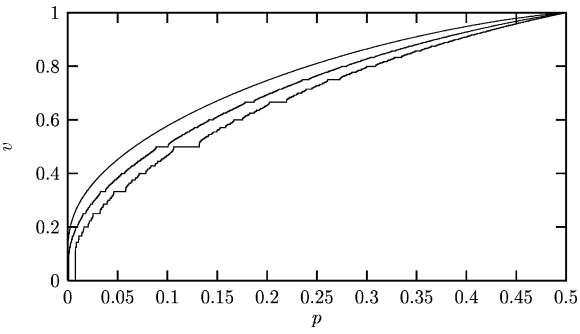

Fig. 3. Comparison of the velocity $v_{\min}$ valid for infinite N (top curve) with the velocity of the model with a cutoff $1/N$ for $N = 512$ (middle curve) and $N = 64$ (bottom curve) as a function of p.

Knowing the function $c(x,t)$ at time t, we generate $c(x,t+1)$. As at time t, all the $x_i(t)$ satisfy

$$x_{\min} \leqslant x_i(t) \leqslant x_{\max},$$

from (14) and (24) the positions $x_i(t+1)$ will lie between $x_{\min}$ and $x_{\max}+1$. The probability p_k that a given particle i will be located at position $x_{\min}+k$ at time $t+1$ is

$$p_k = \big\langle c(x_{\min}+k-1,t+1)\big\rangle - \big\langle c(x_{\min}+k,t+1)\big\rangle \tag{25}$$

with $\langle c(x,t+1)\rangle$ given by (19). Obviously, $p_k \neq 0$ only for $0 \leqslant k \leqslant w$. The probability to have, for every k, n_k particles at location $x_{\min}+k$ at time $t+1$ is given by

$$P(n_0,n_1,\ldots,n_w) = \frac{N!}{n_0!\,n_1!\ldots n_w!}\, p_0^{n_0}\, p_1^{n_1}\cdots p_l^{n_w} \times \delta(N-n_0-n_1-\cdots-n_w). \tag{26}$$

Using a random number generator for a binomial distribution [16], expression (26) allows us to generate the random numbers n_k directly [11].

We have measured from (23) the velocity v_N of the front for several choices of p (0.05, 0.25 and 0.45) and for N ranging from 100 to 10^{16}. Fig. 2 shows the results together with functions $A(p)/\ln^2 N$ given in the next section.

Clearly the apparent power law of Fig. 1 does not persist as N increases and the simulations indicate that $v_{\min} - v_N \sim \ln^{-2} N$ for large N. We are going to see in the next section that this logarithmic correction has a simple origin.

5. Effect of the cutoff

The two main differences between the traveling wave equation (10) and the microscopic model (14) is that the microscopic model is stochastic and that $c(x,t)$ varies by steps multiple of $1/N$ (see (17)).

The effect of the noise is hard to treat analytically and we have not succeeded yet to develop a satisfactory theory for it. The effect of discretization can be however understood rather simply: let us modify (10) by imposing, after each timestep, $c(x,t+1) = 0$ if the value given by (10) is smaller than $1/N$ (in other words, we put a cutoff in the deterministic model to mimic the fact that $c(x,t)$ changes by steps of $1/N$). The velocity v'_N of this deterministic model with a cutoff can be easily measured as under these dynamics the front reaches rapidly a periodic regime [11]. As the cutoff goes to zero (i.e. as N goes to infinity), the speed v'_N converges to the mean-field speed $v_{\min}$ given by (11) and (12). In Fig. 3 we compare this speed for $N = 64$ and $N = 512$ with $v_{\min}$ for $\rho(\alpha)$ given by (24) with $0 \leqslant p \leqslant 0.5$. (One can note that the speed gets locked to rational values as p varies.)

The speed v'_N of this new deterministic model can be calculated analytically [11] for large N:

$$v'_N \simeq v_{\min} - \frac{\pi^2 \gamma_{\min}^2 v''(\gamma_{\min})}{2\ln^2 N}, \tag{27}$$

where $v(\gamma)$ is given by (11). Comparing the prediction (27) with the results of the simulations in Fig. 2 gives a good, though not perfect, agreement. This indicates that the slow convergence of the velocity of the stochastic model is controlled by the effect of the cutoff.

6. Conclusion

We have seen that, for a very particular microscopic stochastic model (14), it was possible to simulate systems of 10^{16} particles. Our model is so particular that there is no hope that our trick could be extended to large classes of statistical physics problems. In our case, however, going to very large N enabled us to clearly discriminate between a power law and a logarithmic correction.

The fact that the microscopic scale selects a single velocity [11,17,18] with a logarithmic correction due to a cutoff seems to appear in several related problems (reaction-diffusion [3,19], kinetic theory [6]). Even model (14) can be introduced in many different contexts, like directed polymers in a random medium (where $x_i(t)$ would be the free energy of a polymer of length t ending at position i), or growth problems (where $x_i(t)$ would be the height variables). Still, we do not know yet whether the prediction (27) based simply on the effect of the cutoff gives the exact large-N behavior of the model (14), or whether a more sophisticated theory is needed to explain the results of Section 5.

Acknowledgements

We thank M. Droz for communicating us several relevant references.

References

[1] R.A. Fisher, The wave of advance of advantageous genes, Ann. Eugenics 7 (1937) 355–369.

[2] A. Kolmogorov, I. Petrovsky, N. Piscounov, Étude de l'équation de la diffusion avec croissance de la quantité de matière et son application à un problème biologique, Bull. Univ. État Moscou A 1 (1937) 1–25.

[3] A.R. Kerstein, Computational study of propagating fronts in a lattice-gas model, J. Statist. Phys. 45 (1986) 921–931.

[4] B. Derrida, H. Spohn, Polymers on disordered trees, spin glasses, and traveling waves, J. Statist. Phys. 51 (1988) 817–840.

[5] J. Cook, B. Derrida, Lyapunov exponents of large, sparse random matrices and the problem of directed polymers with complex random weights, J. Statist. Phys. 61 (1990) 961–986.

[6] R. van Zon, H. van Beijeren, C. Dellago, Largest Lyapunov exponent for many particle systems at low densities, Phys. Rev. Lett. 80 (1998) 2035–2038.

[7] M. Bramson, Convergence of Solutions of the Kolmogorov Equation to Traveling Waves, No. 285 in Memoirs of the American Mathematical Society (AMS, 1983).

[8] M.D. Bramson, Maximal displacement of branching Brownian motion, Comm. Pure Appl. Math. 31 (1978) 531–581.

[9] E.B. Jacob, H. Brand, G. Dee, L. Kramer, I. Langer, Pattern propagation in nonlinear dissipative systems, Physica D 14 (1985) 348.

[10] W. van Saarloos, Front propagation into unstable states. Linear versus nonlinear marginal stability and rate of convergence, Phys. Rev. A 39 (1989) 6367–6390.

[11] E. Brunet, B. Derrida, Shift in the velocity of a front due to a cutoff, Phys. Rev. E 56 (1997) 2597–2604.

[12] U. Ebert, W. van Saarloos, Universal algebraic relaxation of fronts propagating into an unstable state and implications for moving boundary approximations, Phys. Rev. Lett. 80 (1998) 1650–1653.

[13] D.A. Kessler, H. Levine, D. Ridgway, L. Tsimring, Evolution on a smooth landscape, J. Statist. Phys. 87 (1997) 519–544.

[14] H.P. Breuer, W. Huber, F. Petruccione, Fluctuation effects on wave propagation in a reaction-diffusion process, Physica D 73 (1994) 259–273.

[15] H.P. Breuer, W. Huber, F. Petruccione, The macroscopic limit in a stochastic reaction-diffusion process, Europhys. Lett. 30 (1995) 69–74.

[16] W.H. Press, S.A. Teukolsky, W.T. Vetterling, B.P. Flannery, Numerical Recipes in C (Cambridge University Press, 1994).

[17] G.C. Paquette, L.-Y. Chen, N. Goldenfeld, Y. Oono, Structural stability and renormalization group for propagating fronts, Phys. Rev. Lett. 72 (1994).

[18] J. Mai, I.M. Sokolov, V.N. Kuzovkov, A. Blumen, Front form and velocity in a one-dimensional autocatalytic $A + B \to 2A$ reaction, Phys. Rev. E 56 (1997) 4130–4134.

[19] D.A. Kessler, Z. Ner, L.M. Sander, Front propagation: precursors, cutoffs and structural stability, Phys. Rev. E 58 (1998).